Acta Pharmaceutica Sinica B 2018;8(2):200–208

Chinese Pharmaceutical Association
Institute of Materia Medica, Chinese Academy of Medical Sciences

Acta Pharmaceutica Sinica B

www.elsevier.com/locate/apsb
www.sciencedirect.com

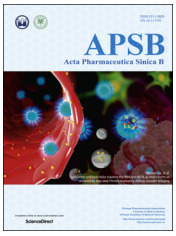

ORIGINAL ARTICLE

Establishment of pseudovirus infection mouse models for *in vivo* pharmacodynamics evaluation of filovirus entry inhibitors

Qing Chen, Ke Tang, Xiaoyu Zhang, Panpan Chen, Ying Guo*

State Key Laboratory of Bioactive Substances and Function of Natural Medicines, Department of Pharmacology, Institute of Materia Medica, Chinese Academy of Medical Sciences, Peking Union Medical College, Beijing 100050, China

Received 26 July 2017; received in revised form 23 August 2017; accepted 28 August 2017

KEYWORDS

Filovirus;
Ebola;
Marburg;
Pseudovirus;
Entry inhibitor;
Mouse model

Abstract Filoviruses cause severe and fatal viral hemorrhagic fever in humans. Filovirus research has been extensive since the 2014 Ebola outbreak. Due to their high pathogenicity and mortality, live filoviruses require Biosafety Level-4 (BSL-4) facilities, which have restricted the development of anti-filovirus vaccines and drugs. An HIV-based pseudovirus cell infection assay is widely used for viral entry studies in BSL-2 conditions. Here, we successfully constructed nine *in vitro* pseudo-filovirus models covering all filovirus genera and three *in vivo* pseudo-filovirus-infection mouse models using Ebola virus, Marburg virus, and Lloviu virus as representative viruses. The pseudo-filovirus-infected mice showed visualizing bioluminescence in a dose-dependent manner. A bioluminescence peak in mice was reached on day 5 post-infection for Ebola virus and Marburg virus and on day 4 post-infection for Lloviu virus. Two known filovirus entry inhibitors, clomiphene and toremiphene, were used to validate the model. Collectively, our study shows that all genera of filoviruses can be well-pseudotyped and are infectious *in vitro*. The pseudo-filovirus-infection mouse models can be used for *in vivo* activity evaluation of anti-filovirus drugs. This sequential *in vitro* and *in vivo* evaluation system of filovirus entry inhibitors provides a secure and efficient platform for screening and assessing anti-filovirus agents in BSL-2 facilities.

Abbreviations: 3D, 3-dimensional; BDBV, Bundibugyo virus; BSL, Biosafety Level; CLO, clomiphene; d.p.i., day post-infection; DLIT, Diffuse Luminescence Imaging Tomography; EBOV, Ebola virus; GP, glycoprotein; h.p.i., hour post-infection; i.p., intraperitoneally; IC_{50}, the 50% inhibitory concentration; lg, logarithm; LLOV, Lloviu virus; MARV, Marburg virus; RAVV, Ravn virus; RESTV, Reston virus; ROI, region of interest; SD, standard deviation; SEM, standard error of the mean; SUDV, Sudan virus; TAFV, Taï forest virus; TORE, toremiphene; VSV-G, vesicular stomatitis virus glycoprotein

*Corresponding author. Tel.: +86 10 63161716; fax: +86 10 63017757.
E-mail address: yingguo6@imm.ac.cn (Ying Guo).

Peer review under responsibility of Institute of Materia Medica, Chinese Academy of Medical Sciences and Chinese Pharmaceutical Association.

http://dx.doi.org/10.1016/j.apsb.2017.08.003

1. Introduction

Filoviruses are enveloped, single-stranded negative-sense RNA viruses. The family *Filoviridae* comprises three genera, *Ebolavirus*, *Marburgvirus*, and *Cuevavirus*[1]. Both ebolaviruses and marburgviruses cause severe human disease, with mortality rates of 24%–90%[2,3]. Cuevavirus is found in bats, and whether it is infectious to humans remains unknown. Ebola virus (EBOV, species *Zaire ebolavirus*) is the most frequently erupting filovirus. It caused the 2013–2015 EBOV epidemic in West Africa, resulting in more than 28,000 suspected cases and 11,310 confirmed deaths[4]. The etiology of Ebola virus disease remains unclear, and new cases appeared in May 2017[5]. Although some vaccines and drugs under study have shown effects[6–8], there are still no licensed anti-filovirus agents available. Filoviruses are select agents and listed as World Health Organization Risk Group 4 Pathogens, for which live virus research requires BSL-4 facilities[9,10], limiting the development of anti-filovirus vaccines and drugs.

Here, we aimed to establish a sequential *in vitro* and *in vivo* filovirus entry inhibitor evaluation system that could be performed in BSL-2 facilities. Because of its safety, pseudovirus based on an HIV-core (pNL4-3.Luc.R^-E^-) is a powerful model for highly pathogenic enveloped viral entry studies *in vitro* (filovirus, highly pathogenic H5N1 influenza virus, severe acute respiratory syndrome coronavirus, Middle East respiratory syndrome coronavirus, and etc.)[11–15]. The bioluminescence imaging assay is a visualizing tool that has been used for viral studies in animal models[16–18]. Although some Ebola virus-like particles used for vaccine studies *in vivo* have been reported[19–21], to the best of our knowledge, there is no study on the comparative *in vivo* pharmacodynamics of filovirus entry inhibitors on different genera of filoviruses. In this study, we constructed nine pseudo-filoviruses, covering all filovirus genera, for screening of filovirus entry inhibitors *in vitro*, and we successfully established three *in vivo* mouse infection models for filovirus entry inhibitor evaluation using the pseudotyped EBOV, Marburg virus (MARV), and Lloviu virus (LLOV) as representative viruses. The robustness of this evaluation system was confirmed by the assessment of two known filovirus entry inhibitors, clomiphene and toremiphene[22]. This sequential *in vitro* and *in vivo* filovirus entry inhibitor evaluation system in BSL-2 conditions will provide powerful technical support for the development of broad-spectrum anti-filovirus agents.

2. Materials and methods

2.1. Cells and plasmids

Human embryonic kidney 293T cells were obtained from the American Type Culture Collection and maintained in Dulbecco's modified Eagle's medium (DMEM) supplemented with 10% fetal bovine serum and 1% penicillin–streptomycin (Invitrogen). The cells were cultured at 37 °C and 5% CO_2. The codon optimized glycoprotein genes (*GP*) of EBOV (EBOV/Mayinga/1976, species *Zaire ebolavirus*, Gene Accession No.AF086833.2), Sudan virus (SUDV/Boniface/1976, species *Sudan ebolavirus*, Gene Accession No.FJ968794.1), MARV (MARV/Musoke/1980, species *Marburg marburgvirus*, Gene Accession No.DQ217792.1), Ravn virus (RAVV/Kenya/1987, species *Marburg marburgvirus*, Gene Accession No.DQ447649.1), and LLOV (LLOV/MS-liver-86/2003, species *Lloviu cuevavirus*, Gene Accession No.JF828358.1) were synthesized and inserted into the pcDNA3.1(+) vector by TSINGKE Biotech (Beijing, China). The *GP* genes of EBOV (EBOV/Makona-Kissidougou-C15/2014, species *Zaire ebolavirus*, Gene Accession No.KJ660346.2), Bundibugyo virus (BDBV/Uganda/2007, species *Bundibugyo ebolavirus*, Gene Accession No.KR063673.1), Taï forest virus (TAFV/Cote d'Ivoire/1994, species *Taï forest ebolavirus*, Gene Accession No.FJ217162.1), and Reston virus (RESTV/Pennsylvania/1989, species *Reston ebolavirus*, Gene Accession No. U23152.1) which inserted into pCMV vector were purchased from Sino Biological Inc. The env-deficient HIV-luc plasmid (pNL4-3. Luc.R^-E^-), which contains a luciferase reporter gene, was obtained from the National Institutes of Health AIDS Research and Reference Reagent Program (Germantown, MD).

2.2. Pseudo-filovirus preparation

Pseudo-filoviruses were produced as previously described[11,13]. Briefly, the plasmids encoding filovirus-GP and the HIV vector (pNL4.3.Luc-R^-E^-) were co-transfected at a 1:1 ratio into 293T producer cells in a 100-mm culture dish using jetPRIME transfection reagent according to the manufacturer's protocol (Polyplus-transfection). Forty-eight hours post-transfection, the HIV/filovirus-GP pseudovirions containing cell culture supernatants were collected and filtered through a 0.45 μm pore size filter (Millipore). Then, for the *in vivo* study, the pseudoviruses were layered onto a cushion of 20% (*w/v*) sucrose and centrifuged at 50,000 rpm for 2 h in a Beckman SW55 rotor at 4 °C. The pelleted pseudoviruses were re-suspended in ice-cold NTE buffer (10 mmol/L Tris, 100 mmol/L NaCl, 1 mmol/L EDTA, pH 7.5) and stored at −80 °C until use. HIV-1 p24 protein in the viral particles was detected by an HIV-1 p24 ELISA kit (Sino Biological Inc.) according to the manufacturer's protocol.

2.3. Viral infection assay and compound activity assay in vitro

293T cells were seeded into 24-well plates at a density of 5×10^4 cells/well. After 24 h, the cells were infected with pseudovirions. Forty-eight hours post-infection, the cells were lysed, and luciferase activity was measured using an FB15 luminometer (Berthold Detection Systems) and a luciferase assay kit (Promega). To detect the *in vitro* anti-filovirus activities of clomiphene citrate (CAS #50-41-9, Sigma–Aldrich) and toremiphene citrate (CAS#89778-27-8, Meilun Inc.), the 293 T cells were incubated with various concentrations of the compounds (0.1–10 μmol/L, three-fold dilution) 15 min prior to infection and then incubated with the pseudoviruses for 48 h. The luciferase activity of the DMSO solvent control was used as the 100% infectivity indicator, and the 50% inhibitory concentration (IC_{50}) of the compound was calculated. Each experiment was repeated three times.

2.4. Animal experiments

Six- to eight-week-old female BALB/c mice (Beijing HFK Bioscience Co., Ltd., Beijing, China) were housed and raised in specific pathogen-free animal facilities of the Institute of Materia Medica (PUMC & CAMS, Beijing, China). Animal research was performed according to the relevant guidelines and regulations and was approved by the Institutional Animal Care and Use Committee of the Institute of Materia Medica (PUMC & CAMS, Beijing, China). Animals were randomly grouped. Animal experimentation was not blinded to the study investigators but was blinded to the

personnel who performed the intraperitoneal injection of pseudovirus solution into mice. Each mouse was inoculated with 0.2 mL pseudovirus solution. For the compound activity experiments, the mice were intraperitoneally (i.p.) administered with different concentrations of compounds, which were dissolved in 0.5% Tween-80/saline with an injection dose of 10 mL/kg, at the time points indicated. Mice in the solvent control group were administered 0.5% Tween-80/saline simultaneously with the drug groups on day –1 and day 0 (–1 h) pre-challenge. For viral challenge, the pseudovirus stocks were diluted in DMEM at the indicated infection dose and administered i.p. at an injection volume of 0.2 mL/mouse. Animal bioluminescence was monitored at the time points indicated, and the body weights of mice were recorded daily until the bioluminescence imaging test was completed.

2.5. *Bioluminescence imaging assay in vivo*

Bioluminescence imaging in mice was conducted using an IVIS Spectrum CT imaging system (PerkinElmer). Briefly, each mouse was injected i.p. with 0.2 mL of a 15 mg/mL solution of D-luciferin potassium salt substrate (XenoLight, PerkinElmer) and anesthetized with isoflurane. Two to five minutes after injection of the substrate, the bioluminescence signals were acquired for 60 s, and the mice were anesthetized during the imaging through nose-cone delivery of isoflurane. To quantify the number of photons emitted from mice, the whole body of the individual mouse was manually defined as the region of interest (ROI), and the relative bioluminescence, which is shown as the total flux (photons/second), was calculated using Living Image 3.0 software (Caliper Life Sciences).

2.6. *Statistical analysis*

The data are expressed as the means ± SEM (standard error of the mean) or SD (standard deviation). Statistical analyses of the comparisons between two groups were performed by unpaired Student's *t*-test using GraphPad Prism 5 software. The statistical significance was set at a P value of <0.05. A P value of <0.05 indicated significant, a P value of <0.01 indicated very significant, and a P value of <0.001 indicated extremely significant.

3. Results

3.1. *Pseudo-filovirus can be used for entry inhibitor evaluation in vitro*

In the filovirus family, EBOV, SUDV, BDBV, TAFV, and RESTV are the members which belong to five species of the *Ebolavirus* genus. RESTV causes asymptomatic infections, and the other four ebolaviruses cause severe and fatal hemorrhagic fever in humans; the *Marburgvirus* genus contains one species, *Marburg marburgvirus*, which includes MARV and RAVV; the *Cuevavirus* genus contains one species, *Lloviu cuevavirus*, with only one member, LLOV. For all filoviruses, the glycoprotein (GP) is the only viral component responsible for entry, and the phylogenetic relationship between filovirus-GPs is shown in Fig. 1A. In this study, we prepared nine HIV-based pseudo-filoviruses covering all species of filovirus. The pseudoviruses were produced by co-transfection of the HIV-core (pNL4-3.Luc. R^-E^-), which contained a firefly luciferase gene, with the filovirus-GP expressing plasmid into 293 T cells. The packaged HIV/filovirus-GP virions had viral envelopes encased with filovirus-GP, which could mediate one-round viral entry into host cells, and the luciferase in infected cells could be used as a reporter for infectivity evaluation. In this system, besides the HIV/filovirus-GP virions, the HIV-alone virions, which had no envelope glycoprotein, and the HIV/VSV-G virions, with the envelope protein of vesicular stomatitis virus glycoprotein (VSV-G), were also prepared as the model controls. The pseudo-filoviruses infecting 293T cells yielded 6 to 8 log signals, and the HIV-alone virions and HIV/VSV-G virions yielded 2 and 8 log signals, respectively (Fig. 1B). Clomiphene and toremiphene, two known filovirus entry inhibitors, were evaluated on these pseudoviruses for system validation. As shown in Table 1, the IC_{50} of clomiphene on filoviruses ranged from 0.28 to 2.26 μmol/L, and the IC_{50} of toremiphene on filoviruses ranged from 0.13 to 3.81 μmol/L; the specificity of the compounds was confirmed by the HIV/VSV-G model (Fig. 1C and D). These results were consistent with the previously reported effects of the compounds on live ebolavirus and marburgvirus[22].

3.2. *Pseudo-filovirus infection in mice can be assessed by bioluminescence imaging*

For the *in vivo* study, the virus collections were purified and condensed by sucrose cushion centrifugation to remove possible immunogenic interference mixtures, such as the serum-containing cell culture media and other cellular metabolites. Then, the amounts of HIV-1 p24 protein of pelleted pseudovirions were quantified by ELISA and used as the measure of viral content.

We first investigated the infection of HIV/EBOV-GP (Mayinga strain, 40 ng p24/mouse) in living mice at the 4th day post-infection (d.p.i.). The inoculation route for mice was intraperitoneal injection, the same route as the live ebolavirus mouse-adapted model in BSL-4 facilities. As shown in Fig. 2A, the bioluminescence in mice infected with HIV/EBOV-GP could be observed; as with uninfected control mice, the HIV-alone virion-infected mice showed no bioluminescence. The photon flux collected from HIV/EBOV-GP-infected mice showed significant differences ($P<0.001$) from that collected from the uninfected control mice (Fig. 2B). The strongest bioluminescence region in mice was on the upper chest, and the 3-dimensional (3D) bioluminescence imaging indicated that the bioluminescence in HIV/EBOV-GP-infected mice mainly accumulated in the thymus (Fig. 2C).

The bioluminescence in HIV/MARV-GP- and HIV/LLOV-GP-infected mice was further monitored. As shown in Fig. 3, these two pseudo-filoviruses could also effectively infect mice, and the bioluminescence localization in mice was identical with the HIV/EBOV-GP group. All pseudo-filovirus-infected mice showed a chronological bioluminescence increase in intensity; after reaching the peak value, the intensity gradually descended. The time point at which the bioluminescence in pseudo-filovirus-infected mice reached the peak differed slightly: for HIV/EBOV-GP and HIV/MARV-GP groups, the peak appeared around 114 h post-infection (h.p.i.), *i.e.*, the 5th d.p.i., while for HIV/LLOV-GP group, the peak appeared around 90 h.p.i., *i.e.*, the 4th d.p.i. In addition, the HIV/EBOV-GP-infected mice showed a higher peak intensity of bioluminescence than the HIV/MARV-GP and HIV/LLOV-GP groups at a 160 ng p24/mouse dose. In order to obtain identical *in vivo* viral infecting levels among pseudo-filoviruses, the viral dose of 40 ng p24/mouse, at which the HIV/

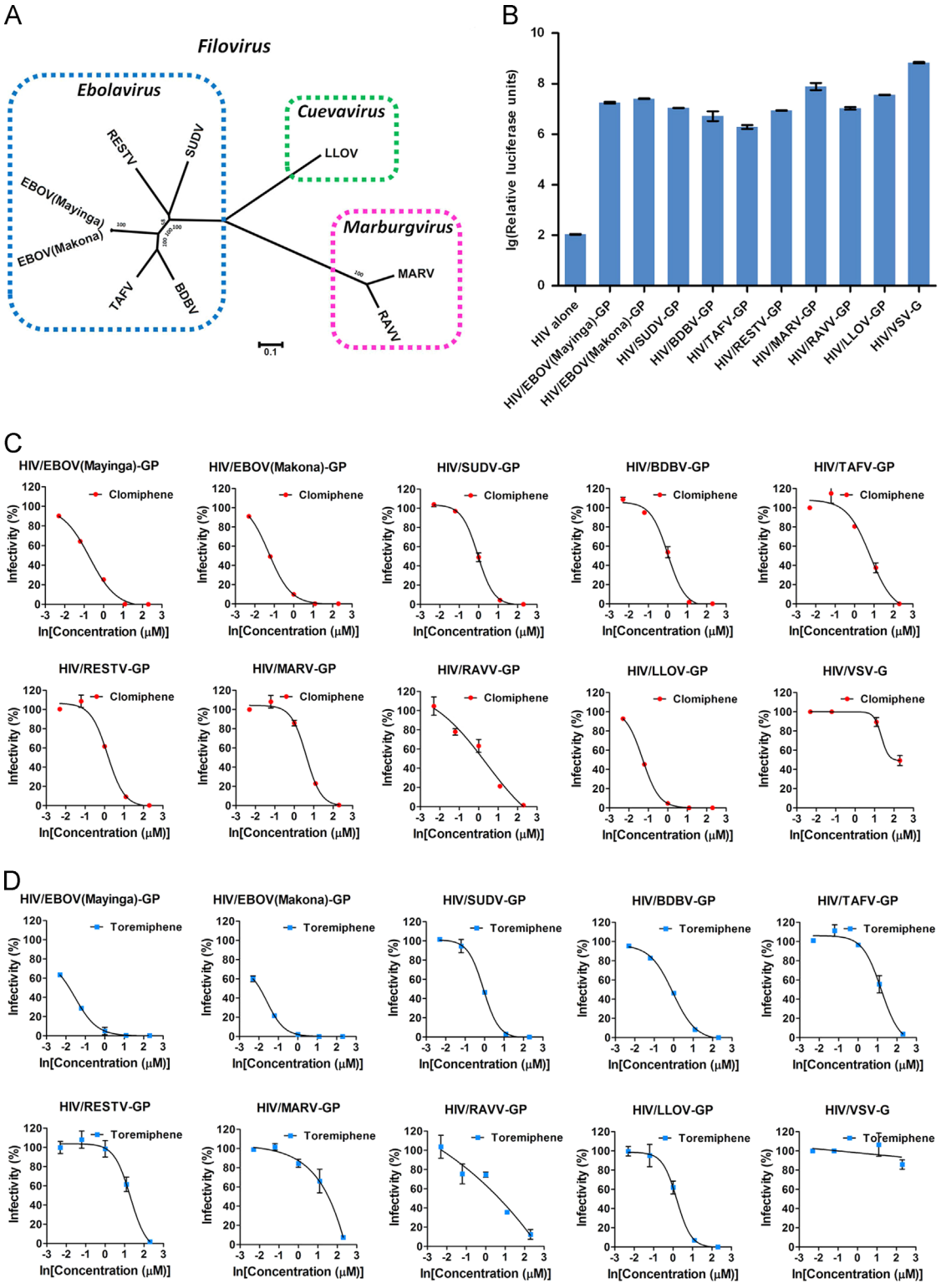

Figure 1 Pseudo-filoviruses can be used for evaluation of entry inhibitors *in vitro*. (A) A phylogenetic tree based on the filovirus-GP protein sequences examined in the present study was generated using MEGA 6.06 software. All species of Filovirus were included. The strains and corresponding gene accession numbers of *GP*s are listed in the Materials and Methods. Construction of the phylogenetic tree was conducted using the neighbor-joining method with 1000 bootstrap replications; the numbers at the nodes indicate the bootstrap values, and the scale bar indicates the number of amino acid substitutions per site. (B) The infectivity of HIV-based pseudo-filovirus in 293T cells was represented as logarithm (lg) of relative luciferase units. HIV-alone represents the pseudovirions without envelope glycoprotein. The data are represented as the average of three independent experiments. Bars, standard deviations. (C) and (D) The effect of clomiphene (C) and toremiphene (D) on HIV/filovirus-GP virus infection in 293T cells. One representative experiment of three is shown. The compounds show dose-dependent inhibition of viral entry for all pseudo-filoviruses but not for HIV/VSV-G viral infection. μM, μmol/L.

Table 1 Effect of clomiphene and toremiphene on HIV/filovirus-GP viruses.

Pseudo-filovirus	Clomiphene		Toremiphene	
	IC_{50} (μmol/L)	95% confidence intervals (μmol/L)	IC_{50} (μmol/L)	95% confidence intervals (μmol/L)
HIV/EBOV(Mayinga)-GP	0.45	0.38 to 0.53	0.15	0.14 to 0.16
HIV/EBOV(Makona)-GP	0.30	0.28 to 0.32	0.13	0.12 to 0.14
HIV/SUDV-GP	0.99	0.97 to 1.00	0.95	0.91 to 0.99
HIV/BDBV-GP	1.04	0.89 to 1.23	0.86	0.74 to 0.99
HIV/TAFV-GP	2.26	1.28 to 3.99	3.23	2.40 to 4.36
HIV/RESTV-GP	1.19	0.88 to 1.62	3.41	2.64 to 4.39
HIV/MARV-GP	1.94	1.47 to 2.55	3.81	2.57 to 5.63
HIV/RAVV-GP	1.56	0.81 to 1.96	1.89	1.04 to 3.45
HIV/LLOV-GP	0.28	0.28 to 0.28	1.19	1.13 to 1.26

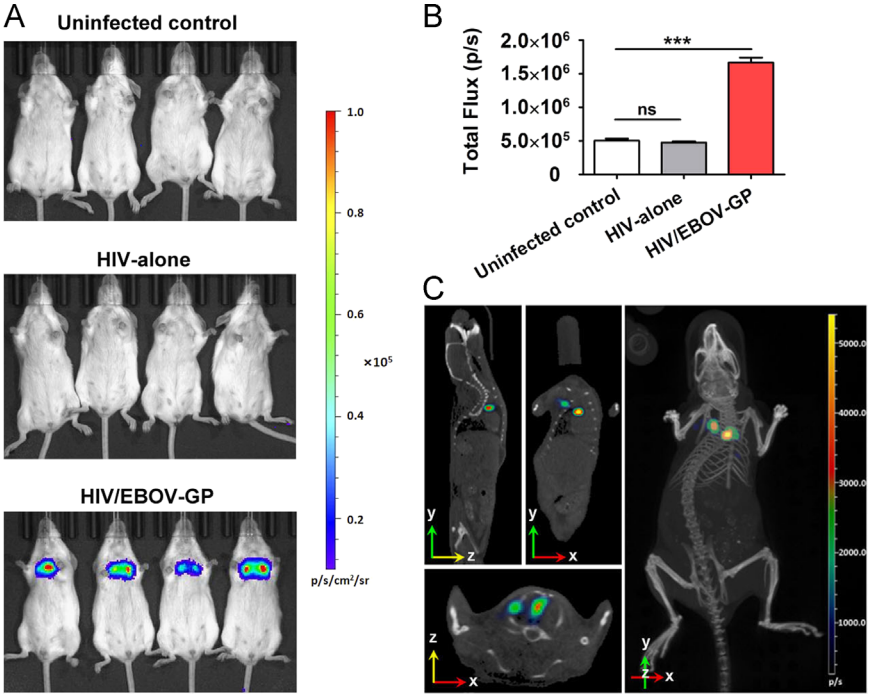

Figure 2 Infection of HIV/EBOV-GP pseudoviruses in BALB/c mice results in bioluminescence *in vivo*. (A) Four days after i.p. inoculation of HIV-alone virions (40 ng p24/mouse) and HIV/EBOV-GP virions (Mayinga strain; 40 ng p24/mouse), the mice were tested with the IVIS Spectrum CT imaging system. All groups, including the uninfected control mice, were i.p. injected with the D-luciferin substrate reagent (p/s/cm^2/sr, photon flux per second per square centimeter per steradian). (B) The bioluminescence intensity of the whole body region of interest (ROI) in mice was represented as total photon flux per second. The data are represented as the means ± SEM ($n=4$ per group). The asterisks represent significant differences: ns, no significance; $^{***}P<0.001$. (C) Representative 3D reconstruction of bioluminescence in HIV/EBOV-GP-infected mice was generated by Diffuse Luminescence Imaging Tomography (DLIT) analysis using the IVIS Spectrum CT imaging system. The 3D imaging was performed at 4 days post-infection. The *x–y, y–z*, and *x–z* axle planes displayed the coronal, sagittal, and transaxial planes, respectively.

EBOV-GP virus showed a comparable bioluminescence intensity to the 160 ng p24/mouse of HIV/MARV-GP and HIV/LLOV-GP infection, was used to further assess the *in vivo* activity of anti-filovirus compounds.

To determine whether the inoculated viral doses correlated with the bioluminescence values of infected mice, linear regression analysis was carried out between the total photon flux in mice and the HIV/EBOV-GP viral doses. As shown in Fig. 4, the bioluminescence in HIV/EBOV-GP-infected mice showed a strong linear correlation with viral dose. The linear bioluminescence-dose correlations were also observed in HIV/MARV-GP- and HIV/LLOV-GP-infected mice (data not shown). The results indicated that the HIV/filovirus-GP infection mouse model could provide accurate assessment of viral infection in living mice.

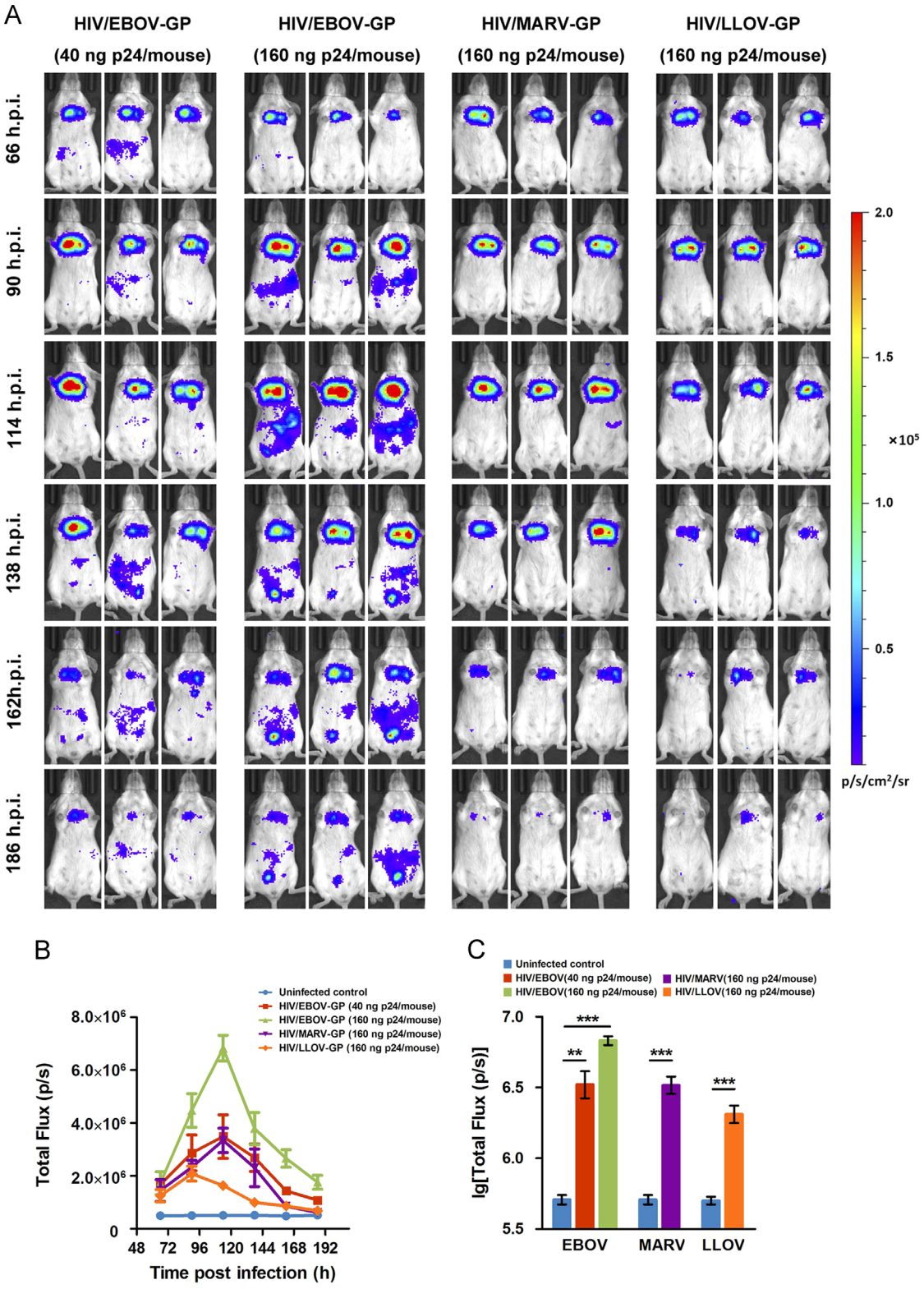

Figure 3 Time scanning of bioluminescence in the HIV/filovirus-GP virus-infected mice. (A) Mice infected with HIV/EBOV-GP (Mayinga strain; 40 ng p24/mouse and 160 ng p24/mouse), HIV/MARV-GP (160 ng p24/mouse), and HIV/LLOV-GP (160 ng p24/mouse) were imaged from 66 to 186 h post-infection (h.p.i.). (B) The values for total flux of whole body ROI in mice at different time points are shown. Each data point represents the mean ± SEM ($n = 3$ per group). The bioluminescence of HIV/EBOV-GP-, HIV/MARV-GP-, and HIV/LLOV-GP-infected mice reached the peak at 114, 114 and 90 h.p.i., respectively. (C) The logarithm values for total flux of mice at the corresponding peak time points of HIV/filovirus-GP groups (HIV/EBOV-GP: 114 h.p.i.; HIV/MARV-GP: 114 h.p.i.; HIV/LLOV-GP: 90 h.p.i.). The statistical differences between virus groups and the uninfected control group were calculated. The asterisks represent significant differences: $^{**}P < 0.01$; $^{***}P < 0.001$.

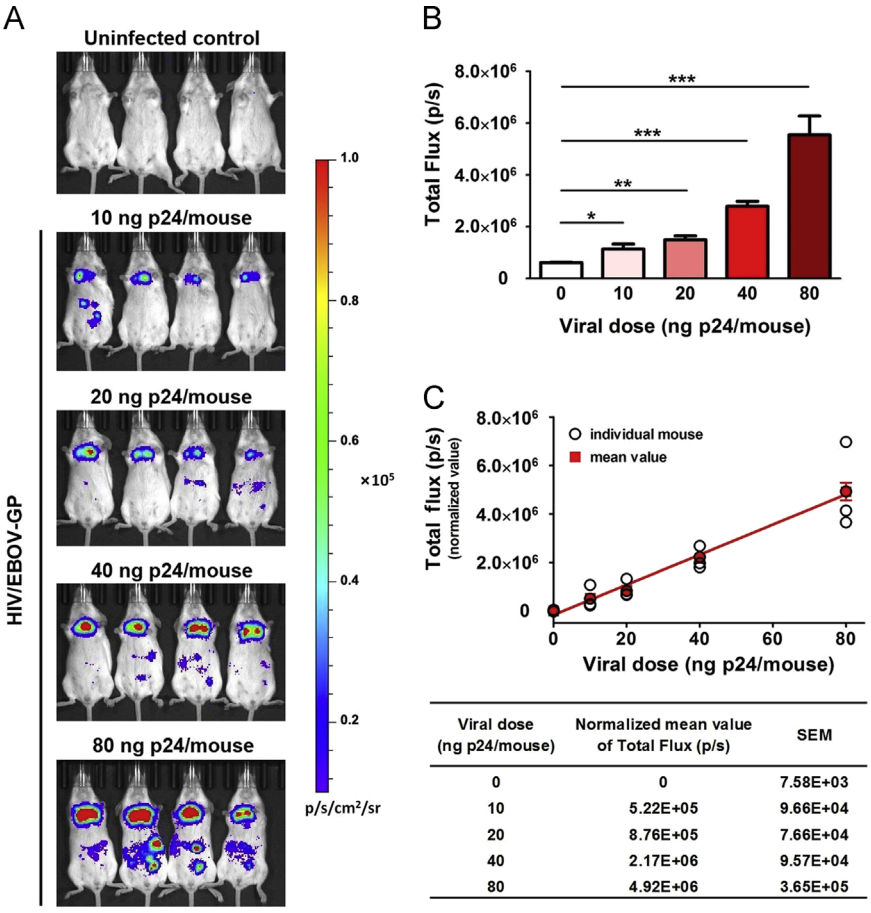

Viral dose (ng p24/mouse)	Normalized mean value of Total Flux (p/s)	SEM
0	0	7.58E+03
10	5.22E+05	9.66E+04
20	8.76E+05	7.66E+04
40	2.17E+06	9.57E+04
80	4.92E+06	3.65E+05

Figure 4 Mice infected with HIV/EBOV-GP viruses showed dose-dependent bioluminescence *in vivo*. (A) Mice infected with different viral doses of HIV/EBOV-GP (Mayinga strain; 10 to 80 ng p24/mouse) were imaged at 114 h.p.i. (B) Values for total flux of whole body ROI in mice are shown. The data are represented as the means ± SEM ($n=4$ per group). The asterisks represent significant differences: $^{*}P<0.05$; $^{**}P<0.01$; $^{***}P<0.001$. (C) The normalized values of total flux, which were obtained by subtracting the mean value of the uninfected control group, are shown. The data showed a strong linear correlation among groups ($R^2=0.9930$).

3.3. Filovirus entry inhibitor activity in vivo can be evaluated by bioluminescence imaging of mice infected with pseudo-filovirus

To validate the *in vivo* model, mice were pretreated with different doses of clomiphene and toremiphene (60, 12, and 2.4 mg/kg of body weight) i.p. once daily on –1 and 0 (–1 h) d.p.i., while the control mice were administered solvent solution (0.5% Tween-80/saline) simultaneously with the compound groups. At day 0, mice were i.p. challenged with HIV/filovirus-GP virions at 40 ng p24/mouse for HIV/EBOV-GP, 160 ng p24/mouse for HIV/MARV-GP, and 160 ng p24/mouse for HIV/LLOV-GP, all in 0.2 mL of DMEM. The bioluminescence in mice was examined at 114 h.p.i. for the HIV/EBOV-GP and HIV/MARV-GP groups and at 90 h.p.i. for the HIV/LLOV-GP group. As shown in Fig. 5, the bioluminescence in both clomiphene- and toremiphene-treated groups presented a dose-dependent inhibition of HIV/EBOV-GP, HIV/MARV-GP, and HIV/LLOV-GP viral infection. The specificity of the two drugs was also confirmed by their inability to inhibit HIV/VSV-G virus *in vivo* (data not shown). These results showed that pseudo-filovirus mouse models can be used for *in vivo* pharmacodynamics evaluation of anti-filovirus compounds.

4. Discussion

Ebolaviruses and marburgviruses were discovered in 1976 and 1967, respectively, but neither anti-filovirus drugs nor vaccines have been approved until now. On the other hand, several agents have been reported to be effective against filovirus infection *in vitro*[7,23], but few of them have been tested *in vivo*, which is partially due to the BSL-4 facilities restriction. The infection of host cells with HIV-based pseudovirus is a single round infection mediated by GP-receptor recognition[23], and expression of the luciferase reporter gene in infected cells or organs can be conveniently used to quantify infection. These features make pseudoviruses a highly secure and efficient model for drug evaluation. Among animal models, the mouse-adapted model is the most widely used for the primary identification of antiviral drugs because of its easy operation and low cost. Therefore, in this study, we established pseudo-filovirus-based *in vivo* mouse models that can be performed in BSL-2 facilities for compound activity evaluation.

For the live virus models, one difficulty is the nonlethal characteristic of wild-type ebolaviruses and marburgviruses in immunocompetent adult mice. Multiple rounds of virus passages

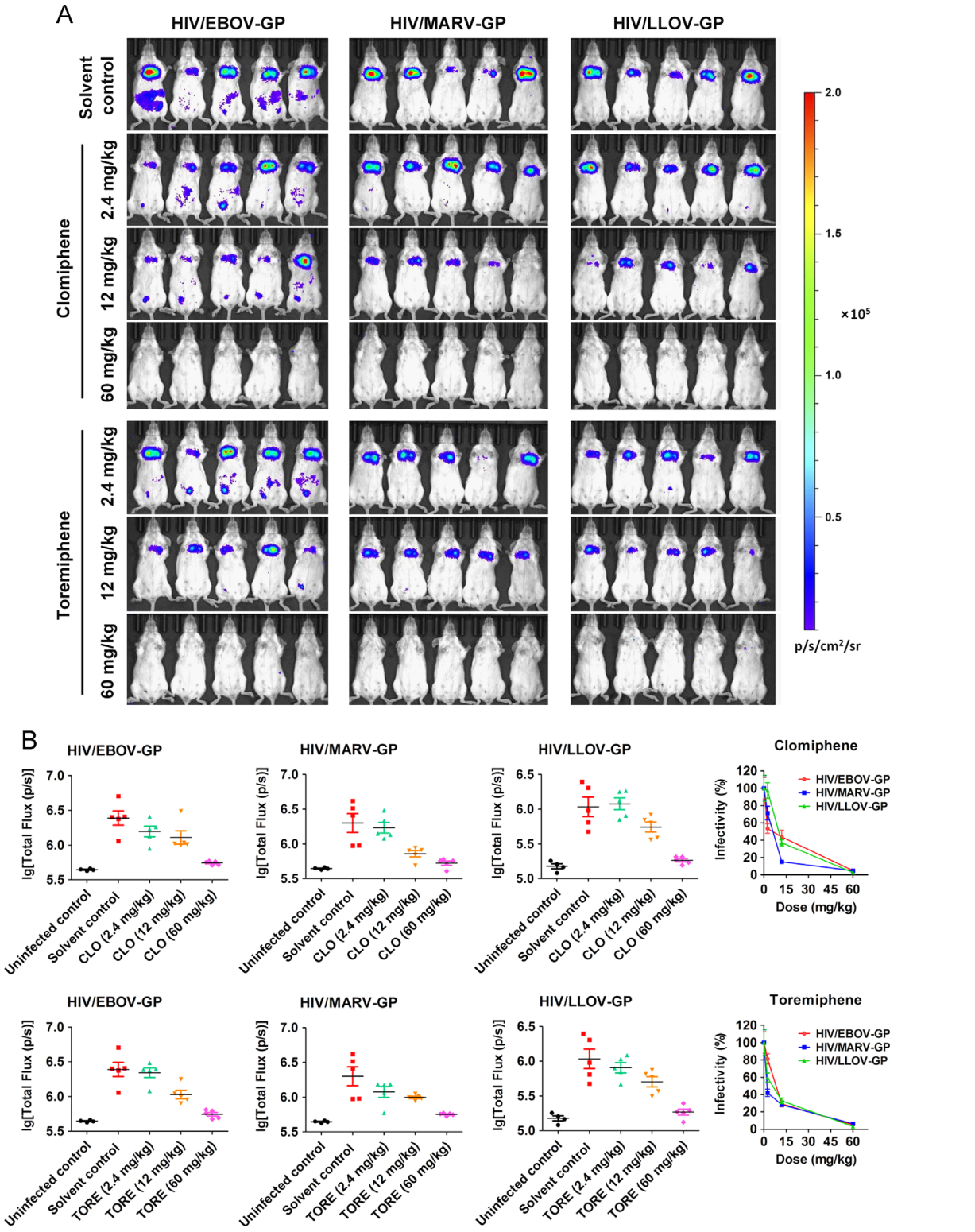

Figure 5 Filovirus entry inhibitors can be evaluated *in vivo* by bioluminescence imaging of mice infected with HIV/filovirus-GP viruses. (A) Mice were i.p. administered with different doses of clomiphene (CLO) and toremiphene (TORE) once daily for two days (–1 and 0 d.p.i.). Bioluminescence was imaged at 114 h.p.i. for the HIV/EBOV(Mayinga)-GPgroup and HIV/MARV-GP group or at 90 h.p.i. for the HIV/LLOV-GP group. (B) The logarithm values for total flux of whole body ROI in mice are shown. The data are represented as the means ± SEM ($n = 5$ per group). The infectivity of the solvent group was set as 100% infection, and the infectivity of the compound groups was calculated. Both CLO and TORE showed a dose-dependent inhibitory effect on HIV/EBOV-GP, HIV/MARV-GP, and HIV/LLOV-GP infection in mice.

had to be conducted and assayed in suckling and immunodeficient mice to obtain the lethal mutant mouse-adapted virus strains for adult mice, and this made the constructions of live ebolavirus and marburgvirus mouse models time-consuming[24,25]. Moreover, it is also difficult to achieve *in vivo* live virus infection models for the virus strains of low pathogenicity and the strains that could be identified only by sequencing. Furthermore, the mutated sites of virus proteins of mouse-adapted virus models might cause some drug candidates to be overlooked, especially small compounds targeting just those sites in wild-type viral proteins. These flaws could be compensated for by pseudo-filovirus *in vivo* models, which could directly use the identical clinically-occurring viral *GP* gene to construct a corresponding *in vivo* imaging model. This would nicely reflect the features of clinically existing viruses and allow for quick response when new types of viruses appear.

5. Conclusions

We established a pseudo-filovirus-based sequential *in vitro* and *in vivo* filovirus entry inhibitor evaluation system that can be performed in BSL-2 facilities. The system covered all genera of filoviruses, including nine pseudo-filovirus *in vitro* models and three bioluminescence imaging *in vivo* mouse models. The verification of two known filovirus entry inhibitors on these models confirmed the success of the model establishments. The high safety, efficiency, and viability of pseudo-filovirus models shed light on anti-filovirus drug research, and this platform can contribute to the discovery of broad-spectrum filovirus entry inhibitors.

Acknowledgments

This work was supported by grants from the National Natural Science Foundation of China (81202568, 81473256, and 81273561), the National Science and Technology Major Project (2015ZX09102-023-004), the CAMS Innovation Fund for Medical Sciences (2016-I2M-1–014), and the Beijing Key Laboratory of New Drug Mechanisms and Pharmacological Evaluation Study (BZ0150).

References

1 Knipe DM, Howley PM. *Fields Virology*. 6th ed. Philadelphia: Lippincott Williams & Wilkins Health; 2013.
2 Feldmann H, Geisbert TW. Ebola haemorrhagic fever. *Lancet* 2011;**377**:849–62.
3 Nyakarahuka L, Kankya C, Krontveit R, Mayer B, Mwiine FN, Lutwama J, et al. How severe and prevalent are Ebola and Marburg viruses? A systematic review and meta-analysis of the case fatality rates and seroprevalence. *BMC Infect Dis* 2016;**16**:708.
4 World Health Organization. Ebola data and statistics [EB/OL]. Last updated: 13 May 2016. Available from: ⟨http://apps.who.int/gho/data/view.ebola-sitrep.ebola-summary-latest?Lang=en⟩.
5 World Health Organization. Ebola virus disease—Democratic Republic of the Congo [EB/OL]. Disease outbreak news: 13 May 2017. Available from: ⟨http://www.who.int/csr/don/13-may-2017-ebola-drc/en/⟩.
6 Qiu X, Audet J, Wong G, Pillet S, Bello A, Cabral T, et al. Successful treatment of Ebola virus-infected Cynomolgus macaques with monoclonal antibodies. *Sci Transl Med* 2012;**4**:138ra81.
7 Kouznetsova J, Sun W, Martínez-Romero C, Tawa G, Shinn P, Chen CZ, et al. Identification of 53 compounds that block Ebola virus-like particle entry *via* a repurposing screen of approved drugs. *Emerg Microbes Infect* 2014;**3**:e84.
8 Wang LL, Chen Q, Zhou LN, Guo Y. Study of gonadal hormone drugs in blocking filovirus entry of cells *in vitro*. *Acta Pharm Sin* 2015;**50**:1545–50.
9 US Department of Health and Human Services. *Biosafety in Microbiological and Biomedical Laboratories (BMBL)*. 5th ed. USA: HHS Publication; 2009.
10 Centers for Disease Control and Prevention. Bioterrorism agents/diseases [EB/OL]. 20 March 2010. Available from: ⟨http://www.bt.cdc.gov/agent/agentlist-category.asp#a⟩.
11 Chen Q, Guo Y. Establishment of a cell-based filovirus entry inhibitor evaluation system. *Acta Pharm Sin* 2015;**50**:1538–44.
12 Ding N, Chen Q, Zhang W, Ren S, Guo Y, Li Y. Structure-activity relationships of saponin derivatives: a series of entry inhibitors for highly pathogenic H5N1 influenza virus. *Eur J Med Chem* 2012;**53**:316–26.
13 Chen Q, Guo Y. Influenza viral hemagglutinin peptide inhibits influenza viral entry by shielding the host receptor. *ACS Infect Dis* 2016;**2**:187–93.
14 Guo Y, Tisoncik J, McReynolds S, Farzan M, Prabhakar BS, Gallagher T, et al. Identification of a new region of SARS-CoV S protein critical for viral entry. *J Mol Biol* 2009;**394**:600–5.
15 de Wilde AH, Jochmans D, Posthuma CC, Zevenhoven-Dobbe JC, van Nieuwkoop S, Bestebroer TM, et al. Screening of an FDA-approved compound library identifies four small-molecule inhibitors of Middle East respiratory syndrome coronavirus replication in cell culture. *Antimicrob Agents Chemother* 2014;**58**:4875–84.
16 Pan W, Dong Z, Li F, Meng W, Feng L, Niu X, et al. Visualizing influenza virus infection in living mice. *Nat Commun* 2013;**4**:2369.
17 Li XF, Li XD, Deng CL, Dong HL, Zhang QY, Ye Q, et al. Visualization of a neurotropic flavivirus infection in mouse reveals unique viscerotropism controlled by host type I interferon signaling. *Theranostics* 2017;**7**:912–25.
18 Nie J, Wu X, Ma J, Cao S, Huang W, Liu Q, et al. Development of *in vitro* and *in vivo* rabies virus neutralization assays based on a high-titer pseudovirus system. *Sci Rep* 2017;**7**:42769.
19 Li D, Chen T, Hu Y, Zhou Y, Liu Q, Zhou D, et al. An Ebola virus-like particle-based reporter system enables evaluation of antiviral drugs *in vivo* under non-biosafety level 4 conditions. *J Virol* 2016;**90**:8720–8.
20 Liu Q, Fan C, Li Q, Zhou S, Huang W, Wang L, et al. Antibody-dependent-cellular-cytotoxicity-inducing antibodies significantly affect the post-exposure treatment of Ebola virus infection. *Sci Rep* 2017;**7**:45552.
21 Zhang L, Li Q, Liu Q, Huang W, Nie J, Wang Y. A bioluminescent imaging mouse model for Marburg virus based on a pseudovirus system. *Hum Vaccin Immunother* 2017;**8**:1–7.
22 Johansen LM, Brannan JM, Delos SE, Shoemaker CJ, Stossel A, Lear C, et al. FDA-approved selective estrogen receptor modulators inhibit Ebola virus infection. *Sci Transl Med* 2013;**5**:190ra79.
23 Martin B, Hoenen T, Canard B, Decroly E. Filovirus proteins for antiviral drug discovery: a structure/function analysis of surface glycoproteins and virus entry. *Antivir Res* 2016;**135**:1–14.
24 Bray M, Davis K, Geisbert T, Schmaljohn C, Huggins J. A mouse model for evaluation of prophylaxis and therapy of Ebola hemorrhagic fever. *J Infect Dis* 1998;**178**:651–61.
25 Qiu X, Wong G, Audet J, Cutts T, Niu Y, Booth S, et al. Establishment and characterization of a lethal mouse model for the Angola strain of Marburg virus. *J Virol* 2014;**88**:12703–14.